have already been described. The distances and angles involved in these bonds are summarized in Table 12. Hydrogen bonding across the centre of symmetry is nearly planar with a separation of the mean planes of the amide groups of 0·37 Å and the hydrogen bonds are effectively linear (Table 12). Between molecules related by **b** translation the bonding deviates markedly from planarity as shown in Fig. 2, the separation of the mean planes of the amide groups is 1·15 Å. This hydrogen bond is far from linear (Table 12). It is of interest to note from Fig. 2 that the bending of the hydrogen atom H(7) out of the amide plane (away from H(4) brings it more into line with the N^{i}–O^{ii} direction.

We are indebted to Dr B. M. Bracher who supplied a copy of the programs *FMLS*, to Professor K. N. Trueblood for the program *MGTL* and to Dr R. E. Cobbledick who adapted both of these programs to the ICL 1909 computer.

References

BLAKE, C. C. F. & SMALL, R. W. H. (1959). *Acta Cryst.* **12**, 417.
BONDI, A. (1964). *J. Phys. Chem.* **68**, 441.
BRACHER, B. H. & TAYLOR, R. I. (1967). U.K.A.E.A. Research Report AERE-R5478.
CRUICKSHANK, D. W. J. (1956). *Acta Cryst.* **9**, 754.
GANTZEL, P. K. & TRUEBLOOD, K. N. (1970). Program *MGTL* (A.C.A. Program No. 1). Chemistry Department, University of California, Los Angeles, California 90024, U.S.A.
International Tables for X-ray Crystallography (1962). Vol. III. Birmingham: Kynoch Press.
LEISEROWITZ, L. & SCHMIDT, G. M. J. (1969). *J. Chem. Soc.* (*A*), p. 2372.
PENFOLD, B. R. & WHITE, J. C. B. (1959). *Acta Cryst.* **12**, 130.
SCHOMAKER, V. & TRUEBLOOD, K. N. (1968). *Acta Cryst.* B**24**, 63.
SMALL, R. W. H. & TRAVERS, S. (1961). *J. Sci. Instrum.* **38**, 205.

Acta Cryst. (1972). B**28**, 2206

The Effect of Molecular Vibrations on Apparent Bond Lengths. III. Diatomic Molecules

BY M. W. THOMAS*

Mathematical Institute, University of Oxford, Oxford, OX1 3LB, England

(*Received* 17 *January* 1972)

A study is made of the effect of the nuclear vibrational motion on the charge density for the isoelectronic series BF, N_2, and CO. Although there are no measurable changes in the positions of the maxima in their dynamic charge densities, there is a reduction in the charge density at these maxima. A simple model for diatomic molecules is introduced to estimate the magnitude of any shift in position and thus any apparent change in bond length. The bond length here is taken to be the distance between the maxima in the charge density such as would be inferred from X-ray measurements. A test of this model on LiH gives a predicted shift of 0·018 a_0 whereas the convolution approximation gives a shift of 0·02 a_0. The variation of shift with vibrational amplitude is also investigated. In this approximation a method is suggested in which one could use the vibrational amplitude and the measured bond shortening to estimate the degree of asphericity in the charge density at the nucleus.

Introduction

In a previous paper (Coulson & Thomas, 1971, which henceforth will be referred to as I), it was shown that some of the differences between the bond lengths measured by X-ray and neutron diffraction methods (Coppens, 1970) can be accounted for by considering the effect of the vibrational motion on the static molecular charge density. Moreover, it was seen in I that a convolution approximation appeared to describe this dynamic charge density adequately near a nucleus. For simple covalent molecules involving hydrogen in which the 1*s* electrons take part in bonding, the effect was significant. This was shown to be the case for diatomics such as H_2 and H_2^+ in I where bond shortenings of 0·1 a_0 were possible and also for simple polyatomics such as water (paper II, Thomas, 1971). However, in other diatomics such as N_2, the 1*s* electrons are not valence electrons and so are not involved in bonding to any great extent. Thus the asphericity in the charge density near the nucleus will be quite small. However, if one looks along the bond axis, there is considerable charge build-up over free spherical atoms both farther into the bond due to the bonding electrons and also farther out of the bond due to the lone pairs. This shows up quite clearly on the difference density map (Bader & Henneker, 1967). Thus it would be

* Present address: Physics Department, University College Cardiff, P.O. Box 78, Cardiff, CF1 1XL, Wales.

interesting to discover whether these charge concentrations affect the dynamic charge density near the nuclei and hence the positions of the maxima.

In a simple picture of chemical bonding one speaks of 'covalent' bonds in which there is charge build-up in the bond and of 'ionic' bonds in which there is charge transfer. In more sophisticated theoretical treatments these notations lose some of their usefulness. Nevertheless, an examination of the charge density for an isoelectronic series shows trends which can be interpreted in terms of charge transfer and charge build-up in the bond. For these reasons the isoelectronic series BF, N_2 and CO is examined in the convolution approximation in the first section. In the second section a simple method is suggested for estimating the order of magnitude of the bond shift from the charge density and the internal vibrational amplitude.

(*a*) *Dynamic charge density for* BF, N_2, Co

For the isoelectronic series BF, N_2, CO, the wave functions for $CO(X^1\sum^+)$ and $BF(X^1\sum^+)$ used were those of McLean & Yoshimine (1967). The wave function for $N_2(X^1\sum_g^+)$ was from Cade, Sales & Wahl (1966). Although calculations have been made at various internuclear distances for these molecules, in this study only wave functions computed at the equilibrium separation R_e have been used. All used extensive basis sets of Slater-type orbitals (STO's) which included *d* and *f* functions. Generally such sets give good one-electron properties. However, the electron density was also computed for CO and BF from a wave function due to Huo (1965). Despite the fact that different exponents were used the charge densities did not differ significantly from those computed from Mc Lean and Yoshimine's wave functions. All the wave functions used are of essentially Hartree–Fock (H–F) quality. The relevant data are summarized in Table 1.

It is convenient at this point to mention the 'cusp' condition (Bingel, 1963; Pack & Byers Brown, 1966) for the charge density at the *j*th nucleus. This is a theoretical condition which any wave function (and hence charge density) must satisfy if it is an exact solution of the (non-relativistic) molecular Hamiltonian. For a diatomic molecule with cylindrical symmetry the 'cusp' condition for the charge density reduces to

$$k_1+k_2=4Q_j. \qquad (1)$$

If the charge density is ϱ then the constants k_1 and k_2 are the ratios $|\partial\varrho/\partial\mathbf{r}|/\varrho$ where $\mathbf{r}$ points into and out of the bond at the *j*th nucleus which has charge Q_j. With this definition k_1 and k_2 are always positive. Approximate values are listed in Table 2 for the isoelectronic series which were obtained by using values of the static charge density $\varrho^e_{R_e}$ at a distance of $0{\cdot}02a_0$

Table 1. *Molecular data*

Molecular constants	Molecules BF	N_2	CO	LiH
Energy (a.u.)	−124·16709	−108·9923	−112·78911	−8·0606
No. of basis functions				
STO's	34	26	34	—
Elliptic	—	—	—	38
Internuclear distance $R_e(a_0)$	2·391	2·068	2·132	3·015
Vibrational frequency (cm^{-1})	1402·1	2358·1	2169·8	1405·67

Table 2. *Constants computed from molecular data*

	BF Boron	N_2 Nitrogen	CO Carbon	CO Oxygen	LiH Hydrogen	H_2	H^+_2
Vibrational constants							
Amplitude fraction C_j	0·6334	0·5	0·5714	0·4286	0·875		
Harmonic oscillator constants							
$A_j(a_0^{-1})$	8·0529	13·260	11·015	14·687	2·0683		
$B_j(a_0^{-2})$	203·73	552·38	381·20	667·69	13·440		
r.m.s. amplitude $\sigma_j(a_0)$	0·05	0·03	0·04	0·03	0·19	0·08	0·11
Charge density slope constants							
Slope constants along bond axis							
Into bond $k_1(a_0^{-1})$	9·04	12·18	10·63	13·66	1·84	1·3	1·4
Out of bond $k_2(a_0^{-1})$	9·11	12·23	10·68	13·72	2·19	2·7	2·6
Slope difference $D=k_2-k_1(a_0^{-1})$	0·07	0·05	0·05	0·06	0·35	1·4	1·2
Slope sum $k_1+k_2(a_0^{-1})$	18·15	24·41	21·31	27·38	4·03	4·0	4·0

from the nucleus. For comparison values for H_2, H_2^+ and LiH are also included.

In the convolution approximation for diatomics, the dynamic charge density in the vicinity of the jth nucleus can be written.

$$\varrho_j(r)=\int \varrho_{R_e}^e(\mathbf{r}-c_j\mathbf{R})\,\varrho^N(R)dR\;(j=1,2) \qquad (2)$$

where $\mathbf{R}=R\mathbf{k}$ and the internuclear distance probability density is $\varrho^N(\mathbf{R})$. The constant c_j will be 0·5 for a homonuclear molecule but in general it depends on which nucleus one is looking at, as

$$c_j=\frac{m_k}{m_1+m_2}\quad\begin{matrix}(j=1,2)\\(k=2,1).\end{matrix} \qquad (3)$$

Here m_1 and m_2 are the nuclear masses. The static charge density, $\varrho_{R_e}^e$ is taken at the equilibrium internuclear distance R_e.

By a simple change of variable $\varrho_j(\mathbf{r})$ can be written in terms of the vibrational distribution of the jth nucleus.

$$\varrho_j(\mathbf{r})=\int \varrho_{R_e}^e(\mathbf{r}-\mathbf{t})\varrho_j^N(t)\mathrm{d}t \qquad (4)$$

Although various nuclear distribution functions are possible, in this study they were all taken to be simple harmonic oscillators in the ground state. Thus the nuclear distributions are of the form

$$\varrho_j^N(t)=A_je^{-B_jt^2}. \qquad (5)$$

The constants A_j and B_j are derived using the spectroscopic frequency ω_e and the constant c_j. The constant B_j is related to the r.m.s. amplitude or vibrational 'half width' σ_j of the jth nucleus

$$\sigma_j=(2B_j)^{-1/2}. \qquad (6)$$

The various constants are given in Table 2. For each molecule, the dynamic charge density along the bond axis was computed using a Romberg integration method.

The results of the computation for BF, N_2 and CO are shown in Figs. 1 to 3 and are summarized in Table 3 where the static and dynamic charge densities at the nuclei are listed.

As one would expect from the discussion of I, the 'cusp' in the static charge density at each nucleus disappeared for each molecule. There were also two other features common to every member of the isoelectronic series. The first is that within the accuracy of the integration, the maxima of the dynamic charge density coincided with those of the static charge density. However, one might have anticipated this result by looking at the slope difference D which is a measure of the asphericity near the nucleus. From Table 2 it is seen that D is much smaller for BF, N_2 and CO than it is for H_2^+, H_2 and LiH. Thus the charge density can be considered to be almost spherical for the isoelectronic series and the shifts will be very small. The second feature is that there is a noticeable reduction in the charge density at the nucleus despite the fact that the vibrational amplitude is small. Again, this can be explained by considering the data of Table 2. The vibrational 'half width' σ_j of carbon in CO is 0·04 a_0 which is much less than the σ_j of a hydrogen in H_2^+ which is 0·11 a_0. Hence one would expect differences between $\varrho(\mathbf{r})$ and $\varrho_{R_e}^e(\mathbf{r})$ in CO only in regions where $\varrho_{R_e}^e(\mathbf{r})$ varies appreciably over distances of the order of 0·04 a_0. This is true in CO only near the nuclei. The values of k_1 and k_2 in Table 2 indicate that the static charge density decreased from 127·07 e.a_0^{-3} at the carbon nucleus to 78·7 e.a_0^{-3} at a distance of 0·04a_0. One might say that the regions in which there is little variation in $\varrho_{R_e}^e$ do not 'feel' the effect of the vibrational motion if σ_j is small. Thus in these regions $\varrho(\mathbf{r})$ will resemble $\varrho_{R_e}^e(\mathbf{r})$ and so features of chemical interest such as 'lone pairs' and 'bond charge' will be retained.

In experimental measurements by X-rays, one in fact often observes a much larger decrease than that which is suggested by Table 3. The reason for this is that the rigid body motion of the molecule also results

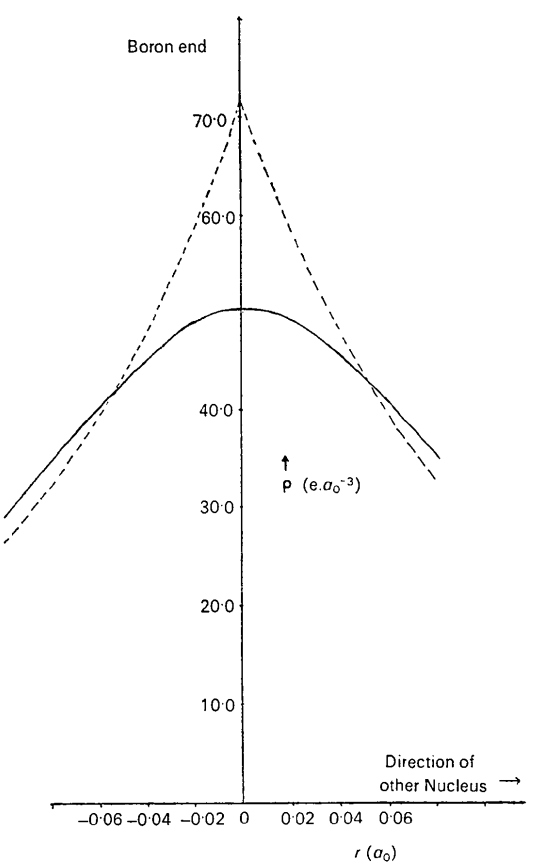

Fig. 1. Static and dynamic charge density for BF: ----static charge density $\varrho_{R_e}^e$; ——dynamic charge densiy ϱ^e.

in a decrease in the apparent charge density at the nucleus. Thus the significance of Table 3 is that even if one corrected for the rigid body motion there would also be a decrease in the charge density due to the internal motion. However, it should be pointed out that experimental determinations of the charge density always have a resolution problem as only a finite set of points in reciprocal space can be sampled.

(*b*) *Estimates of the bond 'shift' for diatomics*

In the previous section it was pointed out that the two factors which determine the dynamic charge density $\varrho(\mathbf{r})$ and hence the bond shift are the vibrational amplitude and the behaviour of $|\nabla\varrho^e_{Re}|$ near the nucleus. However, since the internal vibrational motion for a diatomic is along the bond axis, only the values of ϱ^e_{Re} along this axis will contribute to the integral of equation (4). However, in polyatomics this will not be the case as bending motions will occur, as was shown in II. In fact, as Cruickshank (1956) pointed out, the vibrational motions alone cause apparent bond shortenings, even for atoms with spherical charge distributions.

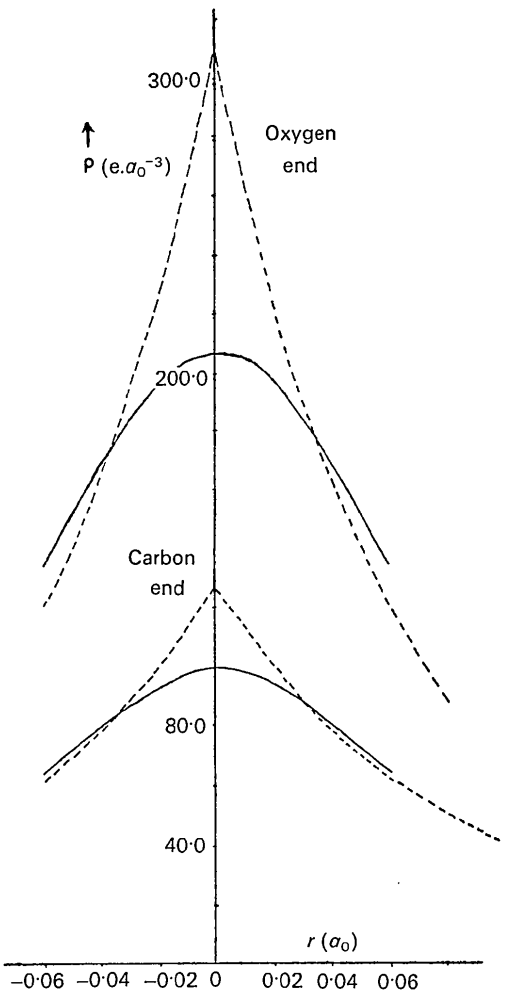

Fig. 2. Static and dynamic charge density for CO: ----static charge density ϱ^e_{Re}; ——dynamic charge density ϱ^e

In a diatomic molecule with a given vibrational distribution, the position of the maximum in $\varrho(\mathbf{r})$ is then determined by the difference in the slope of ϱ^e_{Re} into and out of the bond. This suggests that it may be possible to estimate the position of this maximum by a suitable approximation of $\varrho^e_{Re}(\mathbf{r})$ along the bond axis in the vicinity of the nucleus. One convenient approximation which avoids the numerical integration of $\varrho_j(\mathbf{r})$ is to assume that the static charge density near the jth nucleus can be represented along the bond axis by simple exponentials

$$\varrho^e_{Re} \sim \varrho^e_{Rj}(z) = \begin{cases} K_j e^{-k_1 z} & z > 0 \\ K_j e^{-k_2|z|} & z < 0 \end{cases} \tag{7}$$

The constant K_j is chosen so that the approximation agrees with the static charge density at the nucleus. The slope constants k_1 and k_2 can be chosen so that the approximation agrees with ϱ^e_{Re} at two other points. One possible choice is $\pm\sigma_j$ where σ_j is the 'half width' of the nuclear distribution function $\varrho^N_j(t)$. In general, σ_j will be a measure of the vibrational amplitude. However, if $\varrho^N_j(r)$ is taken to be the simple harmonic oscillator function of equation (5) then σ_j is given by equation (6). In the approximation of equation (7) the integral for the dynamic density ϱ_j along the bond (z axis) can be written

$$\varrho_j(z) = A_j K_j \left\{ \int_{-\infty}^{\circ} \exp\left[k_2 t - \tfrac{1}{2}\left(\frac{z-t}{\sigma_j}\right)^2\right] \mathrm{d}t + \int_{\circ}^{\infty} \exp\left[-k_1 t - \tfrac{1}{2}\left(\frac{z-t}{\sigma_j}\right)^2\right] \mathrm{d}t \right\} \tag{8}$$

where A_j and K_j are constants from equations (5) and (7). The constants k_1 and k_2 depend on σ_j. Equation (8) can be written in the more compact form

$$\varrho_j(z) = A_j K_j [H^{k_1}_j(-z) + H^{k_2}_j(z)] \tag{9}$$

where $H^k_j(x)$ can be written in terms of the complementary error function:

$$H^k_j(x) = \sigma_j \sqrt{\frac{\pi}{2}} \exp\left(kx + \frac{(k\sigma_j)^2}{2}\right) \times \operatorname{erfc}\left[\frac{1}{\sqrt{2}}\left(\frac{x}{\sigma_j} + k\sigma_j\right)\right]. \tag{10}$$

Now the maximum will occur at the point where the derivative of $\varrho_j(z)$ is zero. In the approximation of equation (9) this means that the 'shift' will be the solution near $z = 0$ of the transcendental equation

$$k_1 H^{k_1}_j(-z) = k_2 H^{k_2}_j(z). \tag{11}$$

Since we are considering the vibrational motion to be along the z axis, equation (11) is obtained by differ-

entiating equation (9) with respect to z. The solution, z_0, should give an estimate of the expected shift in the maximum of $\varrho_j(\mathbf{r})$ and hence any bond shortening. Moreover, if the charge is spherically symmetric, then $k_1=k_2$ and from equation (11) one sees that the only solution is $z_0=0$. This indicates there is no shift: this is what one expects. However, even in this case, equation (9) can be used to estimate the decrease in the charge density at the nucleus, which occurs due to the vibrational motion.

In the case that the 'shift' is small compared to the vibrational amplitude σ_j and the slope constants k_1 and k_2, then the function $H_j^k(x)$ of equation (10) can be expanded in powers of x. With this simplification for $H_j^k(x)$ one can replace the transcendental equation for z by an algebraic one which will be correct to some power of z. In general this equation would also be solved numerically. However, in the linear case, $H_j^k(x)$ can be expanded to give

$$H_j^k(x)=\sigma_j\sqrt{\frac{\pi}{2}}\exp(t^2)\operatorname{erfc}(t)$$
$$+[\operatorname{erfc}(t)\sigma_j\sqrt{\frac{\pi}{2}}\exp(t^2)-1]x_k \qquad (12)$$

where $t=k\sigma_{j/\sqrt{2}}$ and $x<\sigma_j$, $x<k$.

In this approximation equation (10) can then be solved for z to give

$$z=\frac{k_1\exp(t_1^2)\operatorname{erfc}(t_1)-k_2\exp(t_2^2)\operatorname{erfc}(t_2)}{k_1^2\exp(t_1^2)\operatorname{erfc}(t_1)+k_2^2\exp(t_2^2)\operatorname{erfc}(t_2)-\sqrt{\frac{2}{\pi}}\left(\frac{k_1+k_2}{\sigma_j}\right)} \qquad (13)$$

where $t_i=k_i\sigma_j/\sqrt{2}$ $(i=1,2)$

The significance of this approximation is that it allows one, in principle, to use the measured bond shortening z to obtain a measure of the asphericity in the charge density at the nucleus. To do this one must also know the 'half width', σ_j, of the vibrational motion of the jth nucleus along the bond axis. If both σ_j and z can be computed from the experimental information then equation (1) can be used to eliminate k_2 from equation (13) and the resulting expression can be solved for k_1. However, it should be pointed out that the constants k_1 and k_2 will now be the slopes at the jth nucleus and not some constants which were chosen to give the best fit to the charge density near the nucleus. Since the slope difference, D, can be taken as a measure of the degree to which the electrons near the nuclei are involved in bonding it is likely to be most important for hydrogen atoms. In fact, the results of the first section suggest it is important only for hydrogen atoms.

In order to test these ideas theoretically, calculations were made for the lithium hydride molecule. Although lithium hydride does not form a molecular crystal it is nevertheless a good molecule for test purposes as it is small enough for very accurate calculations to be made. The wavefunction used in this study was a natural-orbital expansion of Bender & Davidson (1966) in elliptic basis functions. As twelve natural spin-orbitals were used the charge density should be almost exact. The vibrational data was taken from Herzberg (1950). All computations were made for the hydrogen end and the harmonic oscillator approximation was used for the nuclear data. The relevant data are given in Tables 1 and 2.

The spectroscopic frequency gives a 'half width' of 0·1929 a_0. The results using this 'half width' are plotted

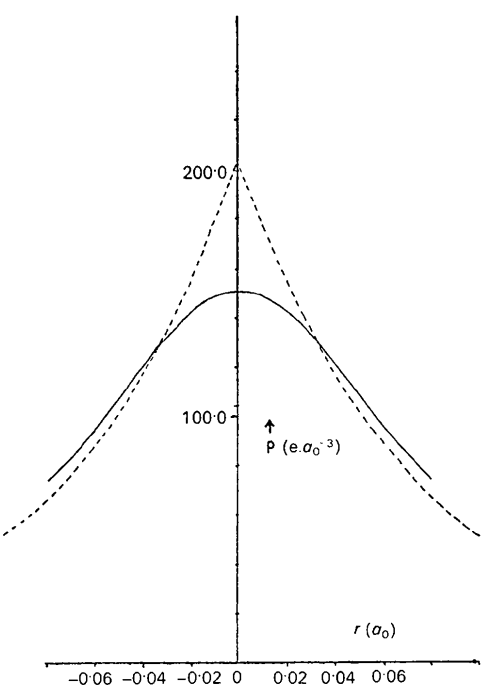

Fig. 3. Static and dynamic charge density for N_2: ----static charge density ϱ_{Re}^e; ——dynamic charge density ϱ^e.

Table 3. *Static and dynamic charge densities at the nuclei*

Charge density	Molecules			
	CO		N_2	BF
Static density $\varrho_{Re}^e(\mathbf{r})$ (e.a_0^{-3})	Carbon 127·07	Oxygen 310·90	Nitrogen 205·59	Boron 71·70
Dynamic density $\varrho(\mathbf{r})$ (e.a_0^{-3})	80·58	196·08	151·41	50·34

in Fig. 4. The graph shows that the exponential approximation ϱ_j^e given by equation (7) reproduces the static charge density ϱ_{Re}^e quite well near the nucleus. This might be expected as the values in Table 2 for k_1 and k_2 near the nucleus were the same as those at $\pm\sigma_j$ to three significant figures. Similarly the shape of the dynamic charge density $\varrho_j(\mathbf{r})$ is approximated quite closely by the exponential model of equation (9) in the vicinity of the nucleus. Moreover the shift predicted by the exponential approximation is 0·018 a_0 which is close to the convolution approximation shift of 0·02 a_0. In fact, as the peak is quite broad it is difficult to estimate the maximum exactly. In an actual crystal the internal vibrational modes of the molecule are often changed through intermolecular coupling. If the change is to lower frequencies then the vibrational amplitudes will increase. There are also large external motions from the lattice modes. Hence one would like to see how well the simple exponential model of equation (9) predicts the 'shift' in the position of the maximum as a function of the vibrational 'half width' σ_j. Again, calculations were made for lithium hydride both with the exponential model of equation (9) and with the convolution approximation of equation (4). The results are plotted on the graph of Fig. 5. When one considers that the peak is quite broad, as is shown in Fig. 4, the agreement between the two is quite good. Also evident is the approximately linear variation of the shift with the half-width parameter σ_j.

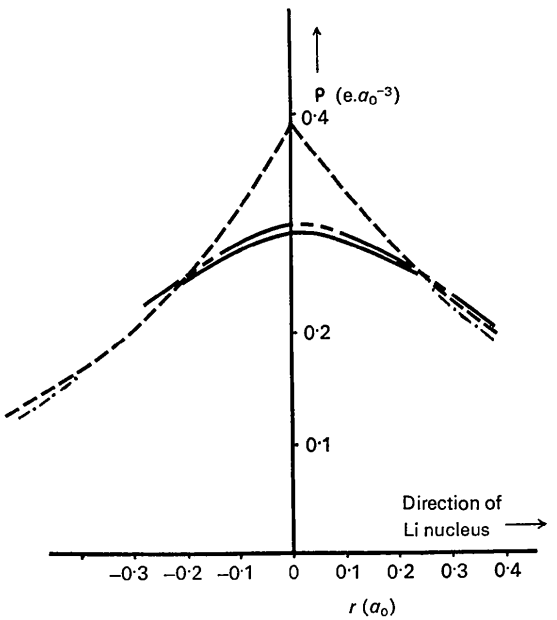

Fig. 4. LiH charge densities (at hydrogen end). Static densities: -----static density, σ_{Re}^e; —·—· exponential fit. Dynamic densities: ——convolution approximating; ·—·—· exponential model.

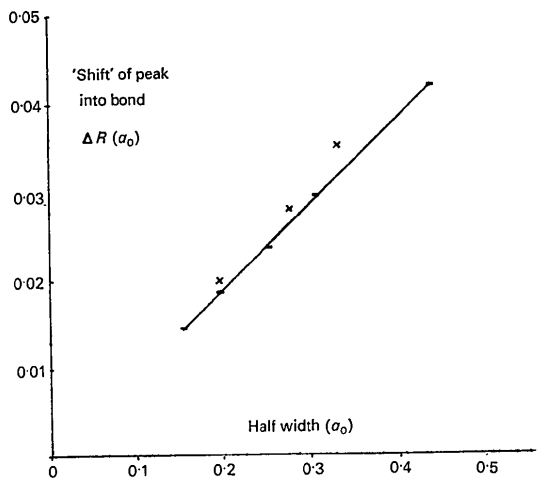

Fig. 5. Variation of 'shift' with vibrational amplitude (LiH, origin at hydrogen atom): × convolution approximation; – exponential model.

In order to check the linear approximation for z which is given by equation (13), calculations for the 'shift' were made using various vibrational 'half-widths' σ_j. The constants k_1 and k_2 were computed by using the value for the static density at $\pm\sigma_j$. The results using equation (13) are listed in Table 4 together with those obtained by solving the transcendental equation [equation (11)].

Table 4. *Bond shortening in* LiH *for various vibrational amplitudes*

'Half' width'	Shift z_o (a_o) (measured from hydrogen equilibrium position)	
$\sigma_j(a_0)$	Exponential model [equation (11)]	Linear exponential model [equation (13)]
0·1547	0·01460	0·01461
0·1786	0·01686	0·01686
0·2188	0·02062	0·02063
0·3094	0·02911	0·02914
0·4375	0·04108	0·04116

Table 4 shows that for LiH the linear approximation gives a bond shortening which agrees very well with the solution of the transcendental equation. In fact, as the peak itself is quite broad these differences are not really significant. Thus the linear approximation for z appears to give the same predicted shifts as the transcendental equation.

As only LiH has been studied it is perhaps unwise to draw any general conclusions. Nevertheless, the results suggest that an estimate of z can be made in terms of k_1, k_2 and σ_j and certain tabulated functions. Moreover, the method appears to give a good estimate of the 'shift' in the maximum of the dynamic charge density not only for the vibrational frequency of the free molecule but also for lower frequencies as well. But it should be mentioned that in an actual crystal the

contribution of the lattice modes will mean that the net nuclear motion is three-dimensional even for a diatomic molecule. Thus the one-dimensional model of equation (9) really considers the effect of the internal vibrational mode of a diatomic molecular crystal.

However, if the X-ray and neutron data were sufficiently accurate that one could estimate the' half-width', σ_j, of the vibrational motion along the bond as well as the bond length shortening, then equations (13) and (1) could be used to find k_1 and k_2. These constants are of interest theoretically as they indicate to what extent the electrons near the nuclei are involved in bonding in the molecule.

References

BADER, R. F. W. & HENNEKER, W. H. (1967). *J. Chem. Phys.* **46**, 3341.

BENDER, O. F. & DAVIDSON, E. R. (1966). *J. Phys. Chem.* **70**, 2675.

BINGEL, W. A. (1963). *Z. Naturforsch.* **18A**, 1249.

CADE, P. E., SALES, K. D. & WAHL, A. C. (1966). *J. Chem. Phys.* **44**, 1973.

COPPENS, P. (1970). *Thermal Neutron Diffraction.* Edited by B. T. M. WILLIS. London: Oxford Univ. Press.

COULSON, C. A. & THOMAS, M. W. (1971). *Acta Cryst.* B**27**, 1354.

CRUICKSHANK, D. W. J. (1956). *Acta Cryst.* **9**, 757.

HERZBERG, G. (1950). *Molecular Spectra and Molecular Structure.* Vol. I. *Spectra of Diatomic Molecules.* Princeton: Van Nostrand.

HUO, W. M. (1965). *J. Chem. Phys.* **43**, 624.

MCLEAN, A. D. & YOSHIMINE, M. (1967). *Tables of Linear Molecule Wave Functions*, Supplement IBM *J. Res. Dev.*

PACK, R. T. & BYERS, BROWN, W. (1966). *J. Chem. Phys.* **45**, 556.

THOMAS, M. W. (1971). *Acta Cryst.* B**27**, 1760.

Acta Cryst. (1972). B**28**, 2212

The Crystal Structure of 3′-Iodobiphenyl-4-carboxylic Acid

BY H. H. SUTHERLAND AND M. J. MOTTRAM*

Physics Department, The University of Hull, England

(*Received* 26 *August* 1971)

The crystal structure of 3′-iodobiphenyl-4-carboxylic acid $C_{13}H_9O_2I$, has been determined from three-dimensional X-ray diffraction data. The crystals are triclinic, space group $P\bar{1}$, with unit-cell dimensions $a=8{\cdot}61$, $b=15{\cdot}92$, $c=4{\cdot}36$ Å, $\alpha=92{\cdot}88$, $\beta=108{\cdot}82$, $\gamma=90{\cdot}00°$. The structure, which consists of centrosymmetrical hydrogen-bonded dimers, was refined by block-diagonal least-squares refinement with anisotropic thermal parameters to a residual of 6% for the 1471 observed structure factors. The molecular geometry is compared with that of related compounds.

Introduction

Halogen substitution in the 2 and 2′ positions of biphenyl has been shown to produce interplanar angles of approximately 50°. As biphenyl in the solid phase is planar it was of interest to study derivatives with halogen in the 3′ position. This paper describes the crystal and molecular structure of 3′-iodobiphenyl-4-carboxylic acid.

Experimental

Slow evaporation from toluene produced transparent yellow platelets, very few of which were suitable for a single-crystal X-ray investigation. The observed density at 19°C was measured by the method of flotation using aqueous cadmium n-dodecatungstaborate. Unit-cell dimensions were obtained from Weissenberg and precession photographs. Crystal data are given in Table 1.

A single crystal of cross section $0{\cdot}018\times0{\cdot}005$ cm perpendicular to the needle axis corresponding to the c axis of the unit cell was selected. Data for the $hk0$, $hk1$, $hk2$ and $hk3$ levels of reciprocal space were collected by the multiple film Weissenberg technique using Mo $K\alpha$ radiation to minimize the effect of absorption. The intensity data for the $0kl$ level were obtained from the same crystal using a precession camera with Mo $K\alpha$ radiation.

Intensities of the spots were measured on a Joyce–Loebl flying-spot densitometer and corrected for Lorentz and polarization factors using the authors' program on an I. C. L. 1905E computer. No correction was applied for absorption.

Determination and refinement of the structure

The $hk0$ projection of the unit cell was solved from the Patterson projection and refined by a combination

* Present address: Procter and Gamble, Newcastle-upon-Tyne, England.